



HAL
open science

Combining regional estimation and historical floods: a multivariate semi-parametric peaks-over-threshold model with censored data

Anne Sabourin, Benjamin Renard

► **To cite this version:**

Anne Sabourin, Benjamin Renard. Combining regional estimation and historical floods: a multivariate semi-parametric peaks-over-threshold model with censored data. *Water Resources Research*, 2016, *Water Resources Research*, 51 (12), pp.19. 10.1002/2015WR017320 . hal-01087687v2

HAL Id: hal-01087687

<https://hal.science/hal-01087687v2>

Submitted on 24 Jan 2016

HAL is a multi-disciplinary open access archive for the deposit and dissemination of scientific research documents, whether they are published or not. The documents may come from teaching and research institutions in France or abroad, or from public or private research centers.

L'archive ouverte pluridisciplinaire **HAL**, est destinée au dépôt et à la diffusion de documents scientifiques de niveau recherche, publiés ou non, émanant des établissements d'enseignement et de recherche français ou étrangers, des laboratoires publics ou privés.



Distributed under a Creative Commons Attribution - ShareAlike 4.0 International License

Combining regional estimation and historical floods: a multivariate semi-parametric peaks-over-threshold model with censored data

November 9, 2015

Manuscript accepted for publication in *Water Resources Research*

Anne Sabourin ¹, Benjamin Renard ²

¹ LTCI, CNRS, Télécom ParisTech, Université Paris-Saclay, 75013, Paris, France
anne.sabourin@telecom-paristech.fr

² Institut National de Recherche en Sciences et Technologies pour l'Environnement
et l'Agriculture, Centre de Lyon
5 rue de la Doua - CS70077, 69626 VILLEURBANNE Cedex, France

Abstract

The estimation of extreme flood quantiles is challenging due to the relative scarcity of extreme data compared to typical target return periods. Several approaches have been developed over the years to face this challenge, including regional estimation and the use of historical flood data. This paper investigates the combination of both approaches using a multivariate peaks-over-threshold model, that allows estimating altogether the intersite dependence structure and the marginal distributions at each site. The joint distribution of extremes at several sites is constructed using a semi-parametric Dirichlet Mixture model. The existence of partially missing and censored observations (historical data) is accounted for within a data augmentation scheme. This model is applied to a case study involving four catchments in Southern France, for which historical data are available since 1604. The comparison of marginal estimates from four versions of the model (with or without regionalizing the shape parameter; using or ignoring historical floods) highlights significant differences in terms of return level estimates. Moreover, the availability of historical data on several nearby catchments allows investigating the asymptotic dependence properties of extreme floods. Catchments display a significant amount of asymptotic dependence, calling for adapted multivariate statistical models.

1 Introduction

Statistical analysis of extremes of uni-variate hydrological time series is a relatively well chartered problem. Two main representations can be used in the context of extreme value theory (*e.g.* *Madsen et al.*, 1997a; *Coles*, 2001): block maxima (typically, annual maxima) can be modeled using a Generalized Extreme Value (GEV) distribution (see *e.g.* *Hosking*, 1985), while flood peaks over a high threshold (POT) are commonly modeled with a Generalized Pareto (GP) distribution (see *e.g.* *Hosking and Wallis*, 1987; *Davison and Smith*, 1990; *Lang et al.*, 1999). One major issue in at-site flood frequency analysis is related to data scarcity (*Neppel et al.*, 2010): as an illustration, most of the recorded flood time series in France are less than 50 years long, whereas flood return periods of interest are typically well above 100 years. Moreover, an additional challenge arises if one is interested in multivariate extremes at several locations. A complete understanding of the joint behavior of extremes at different locations requires to model their dependence structure as well. While there exists a multivariate extreme value theory (*e.g.* *Coles and Tawn*, 1991; *De Haan and De Ronde*, 1998), its practical application is much more challenging than with standard univariate approaches.

1.1 Regional estimation

In order to address the issue of data scarcity in at-site flood frequency analysis, hydrologists have developed methods to jointly use data from several sites: this is known as Regional Frequency Analysis (RFA) (*e.g.* *Hosking and Wallis*, 1997; *Madsen and Rosbjerg*, 1997; *Madsen et al.*, 1997b). The basis of RFA is to assume that some parameters governing the distributions of extremes remain constant at the regional scale (see *e.g.* the 'Index Flood' approach of *Dalrymple*, 1960). All extreme values recorded at neighboring stations can hence be used to estimate the regional parameters, which increases the number of available data.

The joint use of data from several sites induces a technical difficulty: the spatial dependence between sites has to be modeled. A common assumption has been to simply ignore spatial dependence by assuming that the observations recorded simultaneously at different sites are independent, which is often unrealistic (see *Stedinger*, 1983; *Hosking and Wallis*, 1988; *Madsen and Rosbjerg*, 1997, for appraisals of this assumption). Alternative approaches include: (i) using an effective number of stations (*e.g.* *Reed et al.* (1999)) or an effective duration (*Weiss et al.*, 2014); (ii) deriving a multivariate distribution by "skewing" a Gaussian or a Student multivariate distribution (*e.g.* *Ghizzoni et al.* (2012)); (iii) using elliptical copulas (*e.g.* *Renard* (2011) ; *Sun et al.* (2014)). While these approaches allow moving beyond the spatial independence assumption, they do not take full advantage of multivariate extreme value theory (see *e.g.* *Resnick*, 1987, 2007; *Beirlant et al.*, 2004). Indeed, the latter ensures that, when the threshold (*resp.* the block size) increases, the joint distribution of the multivariate excesses (*resp.* the block maxima) converges towards that of a multivariate generalized Pareto distribution (*resp.* a multivariate extreme value distribution). The approach of this paper is to model the joint distribution of excesses using the framework of multi-

variate extreme value theory. As in the univariate case, using such a dependence model is a model choice that finds its justification in the asymptotics (see sections 1.3 and 3 below). It is all the more appropriate that the focus is on out-of-sample quantities, *e.g.* for uncertainty assessments about regional parameters (in particular about shape parameters), and, in turn, about extreme quantiles outside the observational range.

1.2 Historical data

Beside regional analysis methods, an alternative way to reduce uncertainty is to take into account historical flood records to complement the systematic streamflow measurements over the recent period (see *e.g.* *Stedinger and Cohn*, 1986; *O’Connel et al.*, 2002; *Parent and Bernier*, 2003; *Reis and Stedinger*, 2005; *Naulet et al.*, 2005; *Neppel et al.*, 2010; *Payraastre et al.*, 2011; *Machado et al.*, 2015). This results in a certain amount of censored and missing data, so that any likelihood-based inference ought to be conducted using a censored version of the likelihood function. Also, in a regional POT context, some observations may not be concomitantly extreme at each location, so that the marginal GP distribution does not apply to them. A ‘censored likelihood’ inferential framework for extremes has been introduced to take into account such observations (*Smith*, 1994; *Ledford and Tawn*, 1996; *Smith et al.*, 1997). The information carried by partially censored data is likely to be all the more relevant in a multivariate, dependent context, where information at one well gauged location can be transferred to poorly measured ones.

1.3 Multivariate modeling

The family of admissible dependence structures between extreme events is, by nature, too large to be fully described by any parametric model (see further discussion in Section 3.2). For applied purposes, it is common to restrict the dependence model to a parametric sub-class, such as, for example, the Logistic model and its asymmetric and nested extensions (*Gumbel*, 1960; *Coles and Tawn*, 1991; *Stephenson*, 2003, 2009). The main practical advantage is that the censored versions of the likelihood are readily available, but parameters are subject to non-linear constraints and structural modeling choices have to be made *a priori*, *e.g.*, by allowing only bi-variate or tri-variate dependence between closest neighbors. An alternative to parametric modeling is to resort to ‘semi-parametric’ mixture models - some would say ‘non-parametric’ because it can approach any dependence structure - (*Boldi and Davison* (2007); *Sabourin and Naveau* (2014); *Sabourin* (2015), see also *Fougères et al.* (2013) for multivariate models for maxima). In the Dirichlet mixture model that is used in the present work, the distribution function characterizing the dependence structure is written as a weighted average of an arbitrarily large number of simple parametric components. This allows keeping the practical advantages of a parametric representation while providing a more flexible model.

1.4 Objectives: Combining historical data and regional analysis

Our aim is to combine regional analysis and historical data by modeling altogether the marginal distributions and the dependence structure of excesses above large thresholds at neighboring locations with partially censored data. Combined historical/regional approaches have been explored by a few authors (*Tasker and Stedinger*, 1987, 1989; *Jin and Stedinger*, 1989; *Gaume et al.*, 2010; *Viglione et al.*, 2013; *Chi Cong et al.*, 2015). This paper builds on this previous work and extends it to a multivariate POT context, where each d -variate observation corresponds to concomitant streamflows recorded at d sites. This is to be compared with the multivariate annual maxima approach, where each d -variate observation corresponds to componentwise annual maxima that may have been recorded during distinct extreme episodes.

In this paper, a multivariate POT model is implemented in order to combine regional estimation and historical data. This model is used to investigate two scientific questions. Firstly, the relative impact of regional and historical information on marginal quantile estimates at each site is investigated. Secondly, the existence of historical data describing exceptional flood events at several nearby catchments provides an unique opportunity to investigate the nature and the strength of intersite dependence at very high levels (which would be challenging using short series of systematic data only, see *e.g. Serinaldi et al.* (2014)).

Multivariate POT modeling is implemented in a Bayesian, semi-parametric context. The dependence structure is described using a Dirichlet Mixture (DM) model. The DM model was first introduced by *Boldi and Davison* (2007), and its reparametrized version (*Sabourin and Naveau*, 2014) allows for Bayesian inference with a varying number of mixture components. A complete description of the model and of the reversible-jump Markov Chain Monte-Carlo (MCMC) algorithm used for inference with non censored data is given in *Sabourin and Naveau* (2014). The adaptation of the inferential framework to the case of partially censored and missing data is fully described from a statistical point of view in (*Sabourin*, 2015). One practical advantage of this mixture model is that no additional structural modeling choice needs to be made, which allows to cover an arbitrary wide range of dependence structures. In this work, we aim at modeling the multivariate distribution of $d = 4$ locations. However, the methods presented here are theoretically valid in any dimension, and computationally realistic in moderate dimensions (say $d \leq 10$).

The remainder of this paper is organized as follows: the dataset under consideration is described in Section 2, and a multivariate declustering scheme is proposed to handle temporal dependence. Section 3 summarizes the main features of the multivariate POT model and describes the inferential algorithm. In Section 4, the model is fitted to the data and results are described. Section 5 discusses the main limitations of this study and proposes avenues for improvement, while Section 6 summarizes the main findings.

2 Hydrological data

2.1 Overview

The dataset under consideration consists of discharge recorded in the area of the ‘Gardons’, in the south of France. Four catchments (Anduze, 540 km^2 , Alès, 320 km^2 , Mialet, 219 km^2 , and Saint-Jean, 154 km^2) are considered. They are located relatively close to each other (see Figure 1). Discharge data (in $m^3.s^{-1}$) were reconstructed by *Neppel et al.* (2010) from systematic measurements (recent period) and historical floods. *Neppel et al.* (2010) estimated separately the marginal uni-variate extreme value distributions for yearly maximum discharges, taking into account measurement and reconstruction errors arising from the conversion of water levels into discharge. The earliest record dates back to 1604, September 10th and the latest was made in 2010, December 31st.

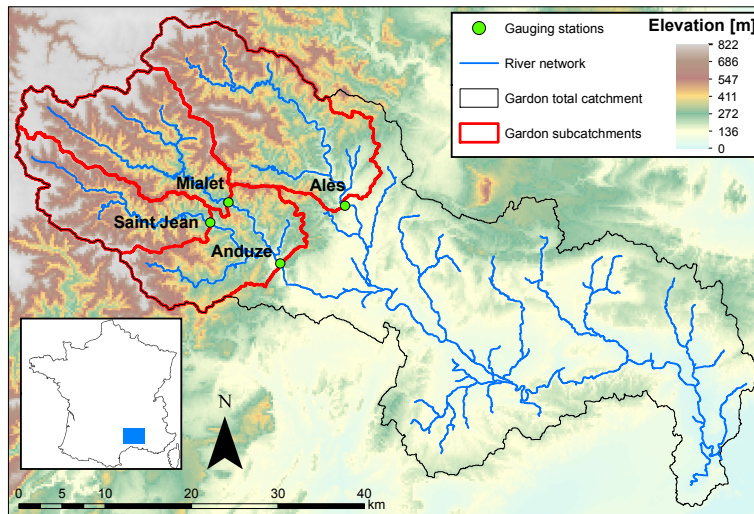


Figure 1: Hydrological map of the area of the Gardons, France

In this work, since we are more interested in the dependence structure between simultaneous records than between yearly maxima, we model multivariate excesses over threshold, and the variable of interest becomes (up to declustering) the daily peakflow. Of course, most of the $N = 14841$ daily peakflows are censored (*e.g.*, most historical data are only known to be smaller than the yearly maximum for the considered year). For the sake of simplicity, we do not take into account any possible measurement errors.

The geographic proximity of the four considered catchments, and the fact that they share broadly similar characteristics (in terms of orientation, shapes, elevations, slopes, geology) suggests that dependence at high levels might be noticeable. This is

visually confirmed by the pairwise plots in Figure 3, obtained after declustering (see Section 2).

The marginal data are classified into four different types, numbered from 0 to 3: ‘0’ denotes missing data, ‘1’ indicate an ‘exact’ record. Data of type ‘2’ are right-censored: the discharge is known to be greater than a given value. Finally, type ‘3’ data are left- and right-censored: the discharge is known to be comprised between a lower (possibly 0) and an upper bound. Most data on the historical period are of type 3. In the sequel, j ($1 \leq j \leq d$) denotes the location index and t ($1 \leq t \leq n$) is used for the temporal one. A marginal observation $O_{j,t}$ is a 4-uple $O_{j,t} = (\kappa_{j,t}, Y_{j,t}, L_{j,t}, R_{j,t}) \in \{0, 1, 2, 3\} \times \mathbb{R}^3$, where κ , Y , L and R stand respectively for the data type, the recorded discharge (or some arbitrary value if $\kappa \neq 1$, which we denote NA), the lower bound (set to 0 if missing), and the upper bound (set to $+\infty$ if missing).

2.2 Data pre-processing: extracting cluster maxima

Temporal dependence is handled by declustering, *i.e.* by fitting the model to cluster maxima instead of the raw daily data. The underlying assumption is that only short term dependence is present at extreme levels, so that excesses above high thresholds occur in clusters. Cluster maxima are treated as independent data to which a model for threshold excesses may be fitted.

Alternative approaches have been investigated for the univariate case, without censored data: in a frequentist context, *Fawcett and Walshaw* (2007) propose to use all the data (not only cluster maxima) and to correct the likelihood with a factor accounting for time dependence, so as to obtain reliable confidence intervals. Alternatively, *Ribatet et al.* (2009) model the whole cluster process within a Markovian model. Both approaches allow using more data for inference and hence reducing uncertainty. However, extending these temporal approaches to the multivariate censored case would require some extra-care, and for the sake of simplicity, the choice was made not to pursue this idea any further in the present paper.

For an introduction to declustering techniques, the reader may refer to *Coles* (2001) (Chap.5). For more details, see *e.g.* *Leadbetter* (1983), or *Davison and Smith* (1990) for applications when the quantities of interest are cluster maxima. Also, *Ferro and Segers* (2003) propose a method for identifying the optimal cluster size, after estimating the extremal index. However, this latter approach relies heavily on ‘inter-arrival times’, which are not easily available in our context of censored data. In this study, we adopt a simple ‘run declustering’ approach, following *Coles and Tawn* (1991) or *Nadarajah* (2001) : a multivariate declustering threshold $\mathbf{v} = (v_1, \dots, v_d)$ is specified (here, $\mathbf{v} = (300, 320, 520, 380)$ respectively for Saint-Jean, Mialet, Anduze and Alès), as well as a duration τ representative of the hydrological features of the catchment (here $\tau = 3$ days). Following common practice (*Coles*, 2001), the thresholds are chosen in regions of stability of the maximum likelihood estimates of the marginal parameters.

In a censored data context, a marginal data $O_{j,t}$ exceeds v_j (*resp.* is below v_j) if $\kappa_{j,t} = 1$ and $Y_{j,t} > v_j$ (*resp.* $Y_{j,t} < v_j$), or if $\kappa_{j,t} \in \{2, 3\}$ and $L_{j,t} > v_j$ (*resp.* $\kappa_{j,t} = 3$ and $R_{j,t} < v_j$). If none of these conditions holds, we say that the data point has undetermined position with respect to the threshold. This is typically the case when

some censoring intervals intersect the declustering thresholds whereas no coordinate is above threshold.

A cluster is initiated when at least one marginal observation $O_{j,t}$ exceeds the corresponding marginal threshold v_j . It ends only when, during at least τ successive days, all marginal observations are either below their corresponding threshold, or have undetermined position. Let $\{t_i, 1 \leq i \leq n_{\mathbf{v}}\}$ be the temporal indices of cluster starting dates. A cluster maximum $\mathbf{C}_{t_i}^{\mathbf{v}}$ is the component-wise ‘maximum’ over a cluster duration $[t_i, \dots, t_i + r]$. Its definition require special care in the context of censoring: the marginal cluster maximum is $C_{j,t_i}^{\mathbf{v}} = (\kappa_{j,t_i}^{\mathbf{v}}, Y_{j,t_i}^{\mathbf{v}}, L_{j,t_i}^{\mathbf{v}}, R_{j,t_i}^{\mathbf{v}})$, with $Y_{j,t_i}^{\mathbf{v}} = \max_{t_i \leq t \leq t_i+r} \{Y_{j,t}\}$ and similar definitions for $L_{j,t_i}^{\mathbf{v}}, R_{j,t_i}^{\mathbf{v}}$. The marginal type $\kappa_{j,t_i}^{\mathbf{v}}$ is that of the ‘largest’ record over the duration. More precisely, omitting the temporal index, if $Y_j^{\mathbf{v}} > L_j^{\mathbf{v}}$, then $\kappa_j^{\mathbf{v}} = 1$. Otherwise, if $L_j^{\mathbf{v}} < R_j^{\mathbf{v}}$, then $\kappa_j^{\mathbf{v}} = 3$; otherwise, if $L_j^{\mathbf{v}} > 0$, then $\kappa_j^{\mathbf{v}} = 2$; If none of the above holds, then the j^{th} cluster coordinate is missing and $\kappa_j^{\mathbf{v}} = 0$.

Figure 2 shows the uni-variate projections of the multivariate declustering scheme, at each location. Points and segments below the declustering threshold indicate situations when the threshold was not exceeded at the considered location but at another one.

Anticipating Section 3, marginal cluster maxima below threshold are censored in the statistical analysis, so that their marginal types are always set to 3, with lower bound at zero and upper bound at the threshold. This approach, fully described *e.g.* in *Ledford and Tawn* (1996), prevents from having to estimate the marginal distribution below threshold, which does not participate in the dependence structure of extremes.

After declustering and censoring below threshold, the data set is made of $n_{\mathbf{v}} = 125$ d -variate cluster maxima $\{\mathbf{C}_{t_i}^{\mathbf{v}}, 1 \leq i \leq n_{\mathbf{v}}\}$. The empirical mean cluster size is $\hat{\tau} = 1.248$, which is to be used as a normalizing constant for the number of inter-cluster days. Namely, m dependent inter-cluster observations contribute to the likelihood as $m/\hat{\tau}$ independent ones would do (see *e.g.* *Beirlant et al.* (2004), Chap. 10 or *Coles* (2001), Chap. 8). As for those inter-cluster observations, $n_{\text{bel}} = 7562$ data points are below thresholds and only 9 days are completely missing (no recording at any location). The remaining $n_{\mathbf{v}}' = 140674$ days are undetermined, and must be taken into account in the likelihood expression. They can be classified into 34 homogeneous temporal blocks (*i.e.* all the days within a given block contain the same information), typically, between two recorded annual maxima.

Figure 3 shows bi-variate plots of the extracted cluster maxima together with undetermined blocks. Exact data are represented by points; One coordinate missing or censored yields a segment and censoring at both locations results in a rectangle. The plots show the asymmetrical nature of the problem under study: the quantity of available data varies from one pair to another (compare, *e.g.*, the number of points available respectively for the pair Saint-Jean/Mialet and Saint-Jean/Alès). Joint modeling of excesses thus appears as a way of transferring information from one location to another. Also, the most extreme observations seem to occur simultaneously (by pairs): They are more numerous in the upper right corners than near the axes, which suggests the use of a dependence structure model for asymptotically dependent data such as

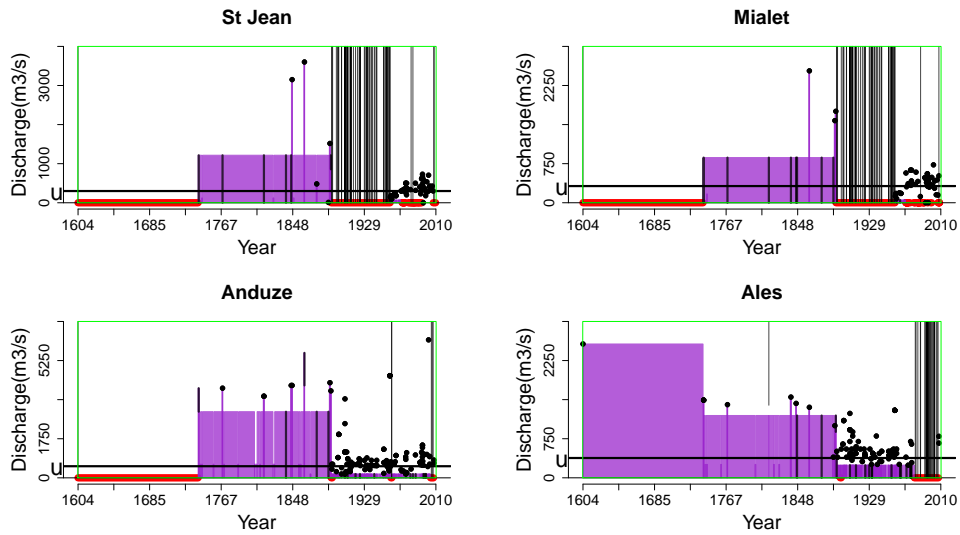


Figure 2: Extracted peaks-over-threshold at the four considered stations. Violet segments and areas represent data of type 2 and 3 available before declustering. Missing days are shown in red. Gray segments (*resp.* black points) are data of type 2 and 3 (*resp.* 1) belonging to an extracted multivariate cluster. In particular, type 2 data are vertical gray segments extending up to the green bounding box. The declustering threshold u is represented by the horizontal black line. Vertical gray lines extending from 0 to the upper limit of the bounding box are drawn at days which are missing at the considered location but which belong to a cluster, due to a threshold excess at another location.

the Dirichlet mixture (see Section 3.2).

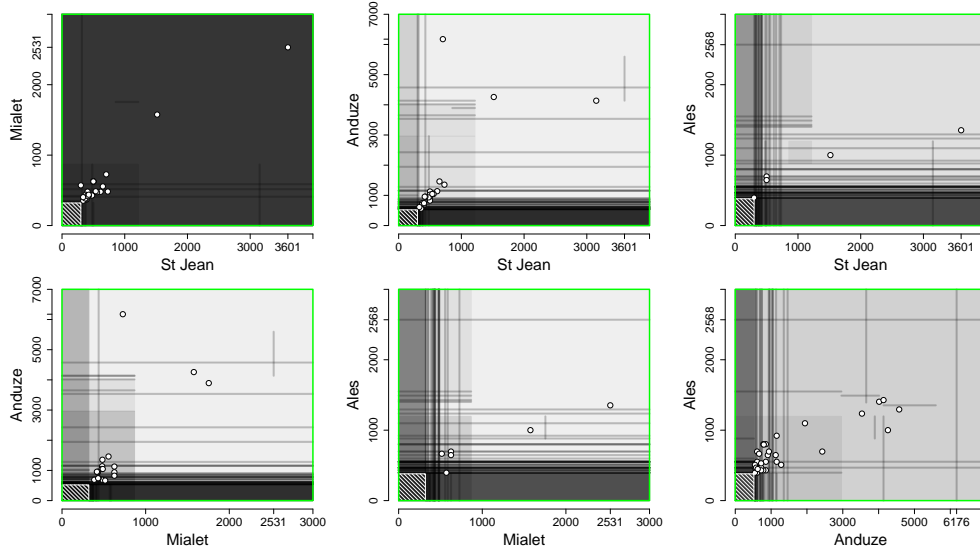


Figure 3: Bi-variate plots of the 124 simultaneous stream-flow records (censored cluster maxima) at the four stations, and of the 34 undetermined data blocks defined in section 2.2, over the whole period 1604-2010. Points represent exact data, gray lines and squares respectively represent data for which one (*resp.* two) coordinate(s) is (are) censored or missing. In particular, gray lines extending throughout the plotting window (green box) indicate a missing coordinate. Data superposition is represented by increased darkness. The striped rectangle at the origin is the region where all coordinates are below threshold.

3 Multivariate peaks-over-threshold model

This section provides a short description of the statistical model used for estimating the joint distribution of excesses above high thresholds. A more exhaustive statistical description is given in the above mentioned paper (*Sabourin, 2015*). For some background about statistical modeling of extremes in hydrology and environmental sciences, the reader may refer *e.g.* to *Katz et al. (2002)*. Also, *Davison and Smith (1990)* focus on the uni-variate case and *Coles and Tawn (1991)* review the most classical multivariate extreme value models. One possible strategy to model joint extremes is to use a parametric model for the joint distribution of POT or block maxima (see *e.g. Cooley et al. (2010); Sabourin et al. (2013)* in a POT context, *Stephenson (2009)* for block maxima, *Salvadori and De Michele (2010)* with a different standardization –uniform margins instead of Pareto margins– leading to representing the dependence *via* an extreme value copula). Alternatively, again in a parametric framework, one may

resort to conditional models for environmental extremes (*Heffernan and Tawn, 2004; Heffernan and Resnick, 2007; Keef et al., 2009*). One advantage of such parametric models is their interpretability; however, using such models requires a-priori modeling choices –and thus modeling errors that are difficult to quantify. Finally, note that for a larger number of locations, and in the case where spatial interpolation is desirable, max-stable models have become increasingly popular over the past few years (*Padoan et al., 2010; Wadsworth and Tawn, 2012; Reich and Shaby, 2012; Davison et al., 2013; Huser and Davison, 2014*). The price to pay for being able to interpolate is, again, a pre-defined parametric dependence structure, and the computational cost. As mentioned in the introduction, the model used here for the dependence structure of extremes is non-parametric (it is a density kernel estimator), so that very little assumption is made regarding the true distribution of the data, and that the produced estimate covers a very wide range of situations.

3.1 Marginal model

After declustering, the extracted cluster maxima are assumed to be independent from each other. Their margins (values of the cluster maxima at each location considered separately) can be modeled by a Generalized Pareto distribution above threshold, provided that the latter is chosen high enough (*Davison and Smith, 1990; Coles, 2001*). Let Y_{j,t_i}^\vee be the (possibly unobserved) maximum water discharge at station j , in cluster i and let F_j^Y the marginal cumulative distribution function (*c.d.f.*) below threshold. The marginal probability of an excess above threshold is denoted ζ_j ($1 \leq j \leq d$). Following common practice (*e.g. Coles and Tawn, 1991; Davison and Smith, 1990; Ledford and Tawn, 1996*), ζ_j is identified with its empirical estimate $\hat{\zeta}_j$, which is obtained as the proportion of intra-cluster days (after uni-variate declustering) among the non-missing days for the considered margin and threshold. For \mathbf{v} as above, it yields $\zeta \simeq (0.0021, 0.0022, 0.0022, 0.0020)$. The estimated standard errors of the estimates range between 2.3×10^{-4} and 3.4×10^{-4} , that is, between 10% and 15% of the estimated values. This error amount was deemed moderate enough to be neglected, compared to the systematic rating curve errors which are discussed in Section 5.1. The marginal models are thus

$$\begin{aligned} F_j^{(\xi_j, \sigma_j)}(y) &= \mathbf{P}(Y_{j,t_i}^\vee < y | \xi_j, \sigma_j), \quad (1 \leq j \leq d) \\ &= \begin{cases} 1 - \zeta_j \left(1 + \xi_j \frac{y - v_j}{\sigma_j}\right)^{-1/\xi} & (\text{if } y \geq v_j), \\ (1 - \zeta_j) F_j^Y(y) & (\text{if } y < v_j). \end{cases} \end{aligned}$$

The marginal parameters are gathered into a $2d$ -dimensional vector

$$\chi = (\log(\sigma_1), \dots, \log(\sigma_d), \xi_1, \dots, \xi_d),$$

and the uni-variate *c.d.f.*'s are denoted by F_j^X .

In a context of regional frequency analysis, it is a popular practice to assume that the shape parameter of the marginal GP distributions is identical for all catchments, i.e. $\xi_1 = \dots = \xi_d$. This assumption is further discussed in Sections 4 and 5.

3.2 Dependence structure

In order to apply probabilistic results from multivariate extreme value theory, it is convenient to handle Fréchet distributed variables X_{j,t_i} , so that $P(X_{j,t_i} < x) = e^{-\frac{1}{x}}$, $x > 0$. This is achieved by defining a marginal transformation

$$\mathcal{T}_j^\chi(y) = -1/\log(F_j^\chi(y)),$$

and letting $X_{j,t_i} = \mathcal{T}_j^\chi(Y_{j,t_i})$. The dependence structure is then defined between the Fréchet-transformed data. Then, under mild assumptions regarding the data's distribution (namely, that the data $\mathbf{Y}_t = (Y_{1,t}, \dots, Y_{d,t})$ are regularly varying, see *e.g.* *Resnick* (1987, 2007); *Beirlant et al.* (2004); *Coles and Tawn* (1991)), we may use two important results from multivariate extreme value theory: in short, the cumulated intensity of the standardized variable \mathbf{X} above high thresholds can be adequately modeled by a Pareto distribution, furthermore, the repartition of the intensity between the different stations is independent from the intensity itself. To get into details, it is convenient to switch to a pseudo-polar coordinates system: let $R = \sum_{j=1}^d X_j$ denote the 'radius' (this is the above mentioned cumulative intensity) and let $\mathbf{W} = (\frac{X_1}{R}, \dots, \frac{X_d}{R})$ denote the angular component of the Fréchet re-scaled data (this is the repartition of the intensity among the stations). In geometrical terms, \mathbf{W} is a point on the simplex \mathbf{S}_d : $\sum_{j=1}^d W_j = 1$, $W_j \geq 0$. The main ingredient of multivariate POT models is that the distribution of the angle given that the radius is large, $\mathbf{P}(\mathbf{W} \in \cdot | R > r_0)$, does converge to a limit distribution, the so-called 'angular probability distribution' of extremes, that we denote by H . Then, for any 'angular region' $B \subset \mathbf{S}_d$, and large enough radial threshold r_0 ,

$$\mathbf{P}(\mathbf{W} \in B | R > r_0) \simeq H(B) \tag{1}$$

Thus, H is the distribution of the angles corresponding to large radii. Since in addition, $\mathbf{P}(R > r_0) \underset{r_0 \rightarrow \infty}{\sim} \frac{d}{r_0}$, the joint behavior of large excesses is entirely determined by H .

As an illustration of this notion of angular distribution, Figure 4 shows two examples of simulated bi-variate data sets, with two different angular distributions and same Pareto-distributed radii. The angular probability density h is represented by the pale red area. In the left panel, h has most of its mass near the end points of the simplex (which is, in dimension 2, the segment $[(1,0), (0,1)]$, represented in blue on Figure 4) and the extremes are weakly dependent, so that events which are large in both components are scarce. In the limit case where H is concentrated at the end-points of the simplex (not shown), the pair is said to be asymptotically independent. In contrast, the right panel shows a case of strong dependence: h is concentrated near the middle point of the simplex and extremes occur mostly simultaneously. Contrary to the limit distribution of uni-variate excesses, H does not have to belong to any particular parametric family. The only constraint on H is due to the standard form of the X_j 's: in the case where H has a density h on the simplex, then it is a valid angular distribution if and only if

$$\int_{\mathbf{S}_d} w_j h(w) dw = \frac{1}{d} \quad (1 \leq j \leq d). \tag{2}$$

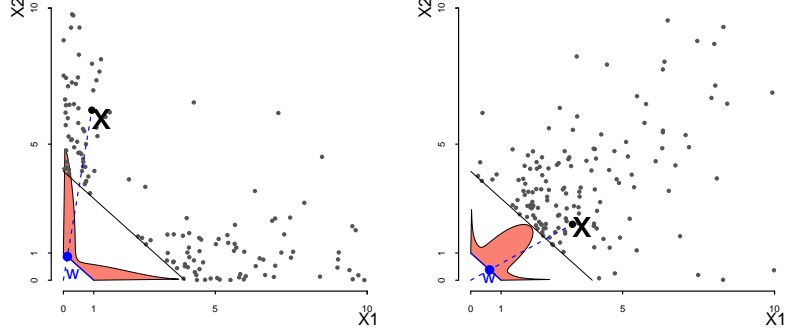


Figure 4: Two examples of bivariate dependence structures of excesses above a radial threshold.

Gray points: simulated bivariate data. Pale red area: density of the angular distribution. Blue point: one randomly chosen angle \mathbf{W} , corresponding to the observation \mathbf{X} (black point). Diagonal solid line: radial threshold (for the norm $\|\mathbf{x}\| = x_1 + x_2$) above which data would typically be considered as extremes

In this paper, h is chosen in the Dirichlet mixture model (*Boldi and Davison, 2007*), which can approach any valid angular distribution. In short, a Dirichlet distribution with shape $\nu \in \mathbb{R}^+$ and center of mass $\boldsymbol{\mu} \in \mathbf{S}_d$ has density

$$\text{diri}_{\nu, \boldsymbol{\mu}}(w) = \frac{\Gamma(\nu)}{\prod_{j=1}^d \Gamma(\nu \mu_j)} \prod_{j=1}^d w_j^{\nu \mu_j - 1}.$$

The density of a Dirichlet mixture distribution is therefore a weighted average of Dirichlet densities. A parameter for a k -mixture is thus of the form

$$\psi = ((p_1, \dots, p_k), (\boldsymbol{\mu}_{\cdot, 1}, \dots, \boldsymbol{\mu}_{\cdot, k}), (\nu_1, \dots, \nu_k)),$$

with weights $p_m > 0$, $\sum_m p_m = 1$, which will be denoted by $\psi = (p_{1:k}, \boldsymbol{\mu}_{\cdot, 1:k}, \nu_{1:k})$. The corresponding mixture density is

$$h_\psi(w) = \sum_{m=1}^k p_m \text{diri}_{\nu, \boldsymbol{\mu}_{\cdot, m}}(w).$$

As for the moment constraint (2), it is satisfied if and only if

$$\sum_{m=1}^k p_m \boldsymbol{\mu}_{\cdot, m} = (1/d, \dots, 1/d). \quad (3)$$

In other terms, the center of mass of the $\boldsymbol{\mu}_{\cdot, 1:m}$'s, with weights $p_{1:m}$, must lie at the center of the simplex.

3.3 Estimation using censored data

Data censorship is the main technical issue in this paper. This section exposes the matter as briefly as possible. For the sake of readability, technical details and full statistical justification have been gathered in *Sabourin (2015)*.

In order to account for censored data overlapping threshold and censored or missing components in the likelihood expression, it is convenient to write the model in terms of a Poisson point process, with intensity determined by h . More precisely, after marginal standardization, the time series of excesses above large thresholds can be described as a Poisson point process (PRM),

$$\sum_{t=1}^n \mathbf{1}_{(t, \mathbf{x}_t)} \sim \text{PRM}(ds \times d\lambda) \quad \text{on } [0, n] \times A_{\mathbf{u}},$$

where n is the length of the observation period, $A_{\mathbf{u}}$ is the ‘extreme’ region on the Fréchet scale, $A_{\mathbf{u}} = [0, \infty]^d \setminus [0, u_1] \times \dots \times [0, u_d]$, above Fréchet thresholds $u_j = \mathcal{T}_j^{\chi}(v_j) = -1/\log(1 - \zeta_j)$. The notation ds stands for the Lebesgue measure and λ is the so-called ‘exponent measure’, which is related to the angular distribution’s density h via

$$\lambda(d\mathbf{x}) = d.h(\mathbf{w})r^{-(d+1)} \quad \left(r = \sum_{j=1}^d x_j, \mathbf{w} = \mathbf{x}/r \right).$$

This Poisson model has been widely used for statistical modeling of extremes (*Coles, 2001; Coles and Tawn, 1991; Joe et al., 1992*). The major advantage in our context is that it allows to take into account the undetermined data (which cannot be ascertained to be below nor above threshold), as they correspond to events of the kind

$$\mathbf{N} \left\{ [t_i, t_i + n_i] \times \left([0, \infty]^d \setminus [0, \mathcal{T}_1^{\chi}(R_{1,t_i})] \times \dots \right. \right. \\ \left. \left. \dots \times [0, \mathcal{T}_d^{\chi}(R_{d,t_i})] \right) \right\} = 0,$$

where $\mathbf{N}\{\cdot\}$ is the number of points from the Poisson process in a given region, t_i is the time of occurrence of n undetermined cluster and n_i is the cluster’s length.

In our context, h is a Dirichlet mixture density: $h = h_{\psi}$. Let $\theta = (\chi, \psi)$ represent the parameter for the joint model, and λ_{ψ} be the Poisson intensity associated with h_{ψ} . The likelihood in the Poisson model, in the absence of censoring, is

$$\mathcal{L}_{\mathbf{v}}(\{\mathbf{y}_t\}_{1 \leq t \leq n}, \theta) \propto e^{-n \lambda_{\psi}(A_{\mathbf{u}})} \prod_{i=1}^{n_{\mathbf{v}}} \left\{ \frac{d\lambda_{\psi}}{d\mathbf{x}}(\mathbf{x}_{t_i}) \times \dots \right. \\ \left. \dots \prod_{j: y_{j,t_i} > v_j} J_j^{\chi}(y_{j,t_i}) \right\}. \quad (4)$$

The J_j^{χ} ’s are the Jacobian terms accounting for the transformation $\mathbf{y} \rightarrow \mathbf{x}$.

The likelihood function in presence of such undetermined data and of censored data above threshold is obtained by integration of (4) in the direction of censorship.

These integrals do not have a closed form expression. In a Bayesian context, a Markov Chain Monte-Carlo (MCMC) algorithm is built in order to sample from the posterior distribution, and the censored likelihood is involved at each iteration. Rather than using numerical approximations, whose bias may be difficult to assess, one option is to use a *data augmentation* framework (see *e.g.* *Tanner and Wong*, 1987; *Van Dyk and Meng*, 2001). The main idea is to draw the missing coordinates from their full conditional distribution in a Gibbs-step of the MCMC algorithm. Again, technicalities are gathered in *Sabourin* (2015).

4 Results

In this section, the multivariate extreme model with Dirichlet mixture dependence structure is fitted to the data from the Gardons, including all historical data and assuming a regional shape parameter. To assess the impact and the potential added value of taking into account historical data on the one hand, and of a regional analysis on the other hand, inference is also made without the regional shape assumption and considering only the systematic measurement period (starting from January, 1892). Thus, in total, four model fits are performed.

For each of the four experiments, 6 chains of 10^6 iterations are run in parallel, which requires a moderate computation time – The execution time ranged from approximately 3h30' to 4h30' for each chain on a standard processor Intel 3.2 GHz. Using parallel chains allows to check convergence using standard stationarity and mixing tests (*Heidelberger and Welch* (1983)'s test, *Gelman and Rubin* (1992)'s variance ratio test), available in the R statistical software. In the remainder of this section, all posterior predictive estimates are computed using the last $8 * 10^5$ iterations of the chain obtaining the best stationarity score.

4.1 Estimations based on the marginal distributions

The regional hypothesis (identical shape parameter across stations) is confirmed (not rejected) by a likelihood ratio test performed in a preliminary analysis: the p-value of the χ^2 statistic is 0.16. It should be noticed that the latter test was performed under the simplifying assumption that the stations were independent, which simplifies the expression for the likelihood –the latter reduces to a product of marginal contributions. For illustrative purposes, the regional shape hypothesis was retained in the subsequent analysis. However, it should be considered with care, since it has a significant impact both on posterior distributions of marginal parameters (Figure 5) and on predicted return levels (Figure 6). A possible refinement for this model choice procedure is discussed in Section 5.2. We emphasize that our goal in the present paper is not to validate the ‘regional shape parameter’ model against the ‘at-site shape parameter’ model, but rather to show that any of these two marginal models may be used in combination with a dependence structure model as described in Section 3.

Figure 5 shows posterior histograms of the marginal parameters, together with the prior density. The posterior distributions are much more concentrated than the priors,

indicating that marginal parameters are identifiable in each model. Also, the shape and scale panels are almost symmetric: a posterior distribution granting most weight to comparatively high shape parameters concentrates on comparatively low scales. This corroborates the fact that frequentist estimates of the shape and the scale parameter are negatively correlated (*Ribereau et al.*, 2011). In the regional model as well as in the local one, the posterior variance of each parameter is reduced when taking into account historical data (except for the scale parameter at Anduze, for the local model). This confirms the general fact that taking into account more data tends to reduce the uncertainty of parameter estimates.

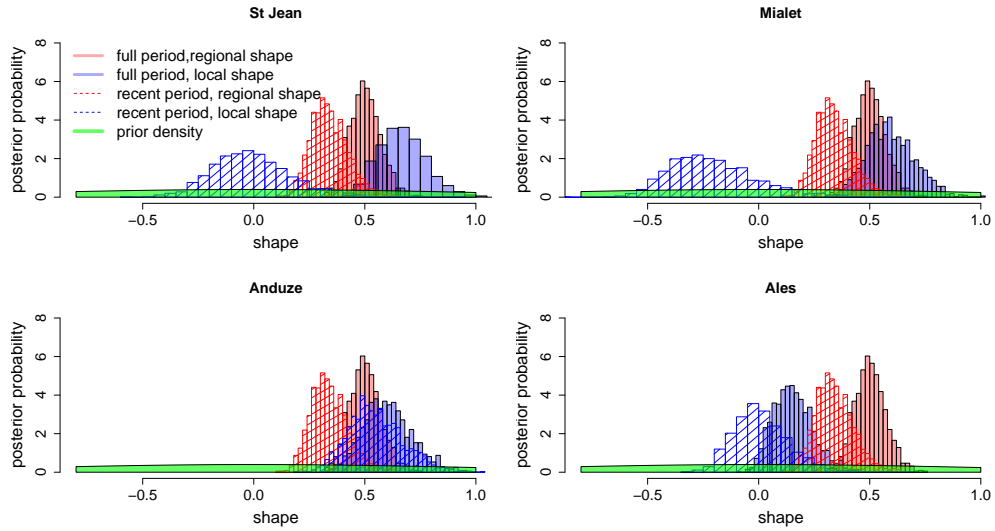
Figure 6 shows posterior mean estimates of the return levels at each location, together with credible intervals based on posterior 0.05 – 0.95 quantiles, in the four inferential frameworks. The return levels appear to be very sensitive to model choice: overall, taking into account the whole period increases the estimated return levels. In terms of mean estimate, the effect of imposing a global shape parameter varies from one station to another, as expected. For those return levels, the posterior credibility intervals seem to depend more on the mean return levels than on the choice of a regional or local framework. This seems at odds with the previous findings of reduced intervals for marginal parameters. However, one must note that the width of return level credibility intervals depends not only on that of the parameters, but also on the value of the mean estimates. In particular, larger estimates on the shape parameter involve larger uncertainties in terms of return levels.

Considering Figure 5 and Figure 6 together allows assessing the effect of each information type on parameter and quantile estimates. First, Figure 6 suggests that all four models yield similar estimates for small to moderate return periods (10-year order of magnitude), but strongly diverge for high quantiles (100-year and above). The largest discrepancies occur for St Jean and Mialet catchments between the two local estimation schemes (recent and full periods). With recent data only, the posterior pdf of the shape parameter is concentrated on negative values, thus suggesting a light-tailed distribution (blue hatched histograms in Figure 5). When the full period is considered, this posterior pdf moves to high positive values, suggesting a heavy-tailed distribution (blue histograms in Figure 5). The effect on quantiles is very strong, with the “recent period” quantile curve (blue hatched curves in Figure 6) being much lower than, and mostly incompatible with, the “full period” quantile curve (blue curves in Figure 6).

The “true” distribution remaining unknown, it is difficult to provide a definitive explanation for these differences. However, the estimates based on the recent period likely lead to underestimating the tail of the distribution, due to an abnormally low number of extreme floods. We based this claim on the following two observations:

- The inclusion of regional information favors the “heavy-tailed” assumption, and we note that as soon as regional and/or historical information is used, the posterior pdfs from the different estimation schemes are compatible with each other. By contrast, the “local, recent period” estimates, which use neither regional nor historical information, stand out.
- Several studies in the French Mediterranean area suggest that both precipita-

Shapes



Scales

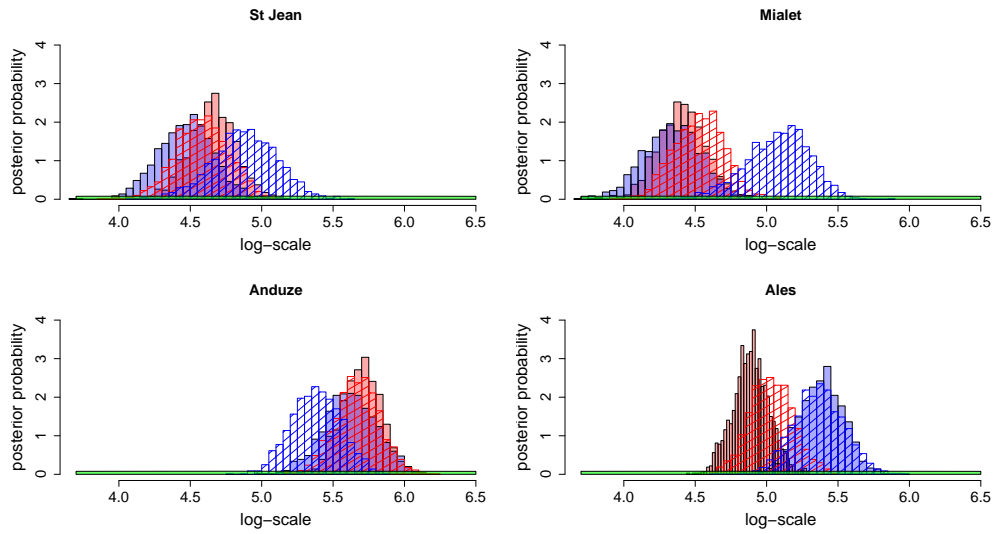


Figure 5: Prior and posterior distributions of the shape parameter (upper panel) and of the logarithm of the scale parameter (lower panel) at the four locations, estimated with or without historical data, in a regional framework or not.

N.B. the historical period extends from 1604/09/10 to 1891/12/31 ; the recent one extends from 1892/01/01 to 2010/12/31.

tion and streamflow extremes follow heavy-tailed distributions (*Neppel et al.*, 2007; *Kochanek et al.*, 2014; *Neppel et al.*, 2014). In addition, the specific discharges for the “local, recent period” estimates of the 100-year flood are below $5 \text{ m}^3 \cdot \text{s}^{-1} \cdot \text{km}^{-2}$, which seems quite small in this region where specific discharges generally lie in the $5\text{-}10 \text{ m}^3 \cdot \text{s}^{-1} \cdot \text{km}^{-2}$ range (*Neppel et al.*, 2010).

4.2 Estimations based on the joint distribution

In addition to uni-variate quantities of interest such as marginal parameters or return level curves, having estimated the dependence structure gives access to multivariate quantities.

Figure 7 shows the posterior mean estimates of the angular density. Since the four-variate version of the angular distribution cannot be easily represented, the bivariate marginal versions of the angular distribution are displayed instead. Here, the unit simplex (which was the diagonal blue segment in Figure 4) is represented by the horizontal axis, so that h is a probability density function on $[0, 1]$. As could be expected in view of Figure 3, extremes are rather strongly dependent. Moreover, the posterior distribution is overall well concentrated around the mean estimate.

The predictive angular distribution allows estimating conditional or joint probabilities of exceedance of high thresholds. This estimation is of interest for at least two reasons:

1. This allows checking the dependence model, by comparing model-computed conditional/joint probabilities with the corresponding conditional/joint frequencies;
2. Such conditional/joint probabilities have a practical interest, in particular for stakeholders managing several catchments. For instance, a flood event simultaneously affecting two catchments does not involve the same response strategy than managing two distinct events affecting a single catchment at a time. The former case requires computing the joint (or alternatively the conditional) probability of occurrence.

As an example, figure 8 displays, for the six pairs $1 \leq j < i \leq 4$, the posterior estimates of the conditional tail distribution functions $P(Y_i^\vee > y | Y_j^\vee > v_j)$ at location i , conditioned upon an excess of the threshold v_j at another location j . The predictive tail functions in the DM model concur with the empirical estimates for moderate values of y . For larger values, the empirical error grows and no empirical estimate exists outside the observed domain. However, the DM estimates are still defined and the size of the error region remains comparatively small.

Finally, one commonly used measure of dependence at asymptotically high levels between pairs of locations is defined by (*Coles et al.*, 1999):

$$\begin{aligned} \chi_{i,j} &= \lim_{x \rightarrow \infty} \frac{P(X_i > x, X_j > x)}{P(X_j > x)} \\ &= \lim_{x \rightarrow \infty} P(X_i > x | X_j > x), \end{aligned}$$

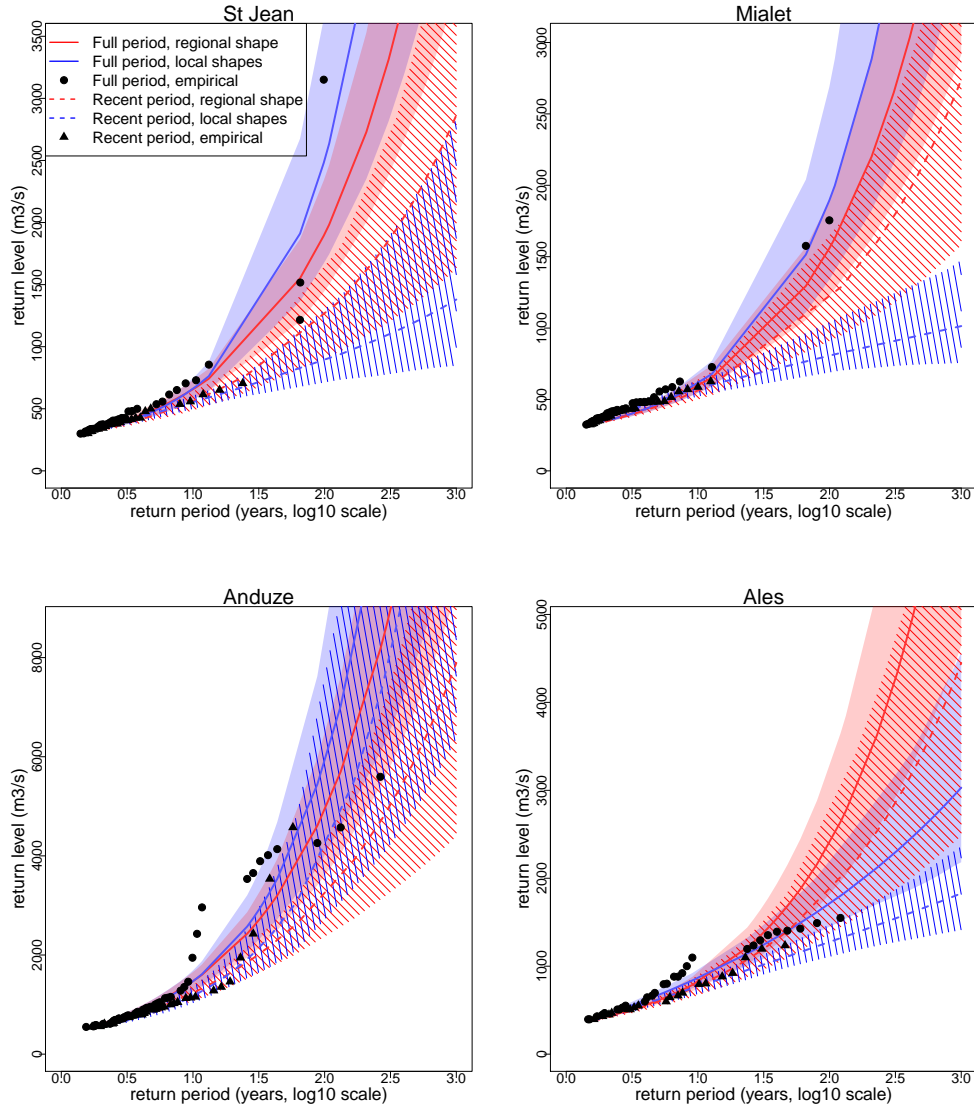


Figure 6: Return level plots at each location using four inferential frameworks with 90% posterior quantiles. Dotted lines and hatched areas: data from the recent period only (from 1892/01/01 to 2010/12/31); Solid lines and shaded area: Full data set (from 1604/09/10 to 2010/12/31); Red lines and pale red area: Regional analysis, global shape parameter; Blue lines and pale blue area: local shape parameters. Black circles (*resp.* triangles): observed data plotted at the corresponding empirical return period using the whole (*resp.* recent) data set.

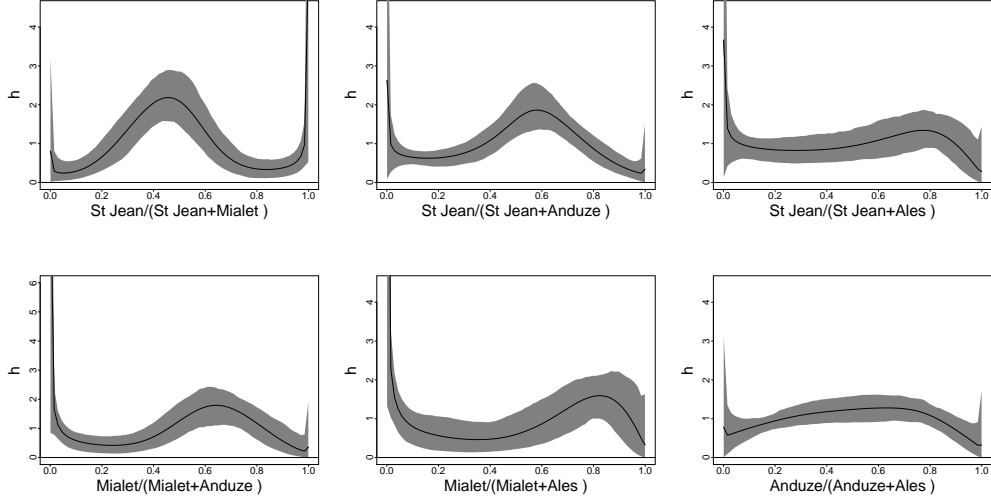


Figure 7: Posterior predictive bi-variate angular densities (black lines) with posterior 0.05 – 0.95 quantiles (gray areas).

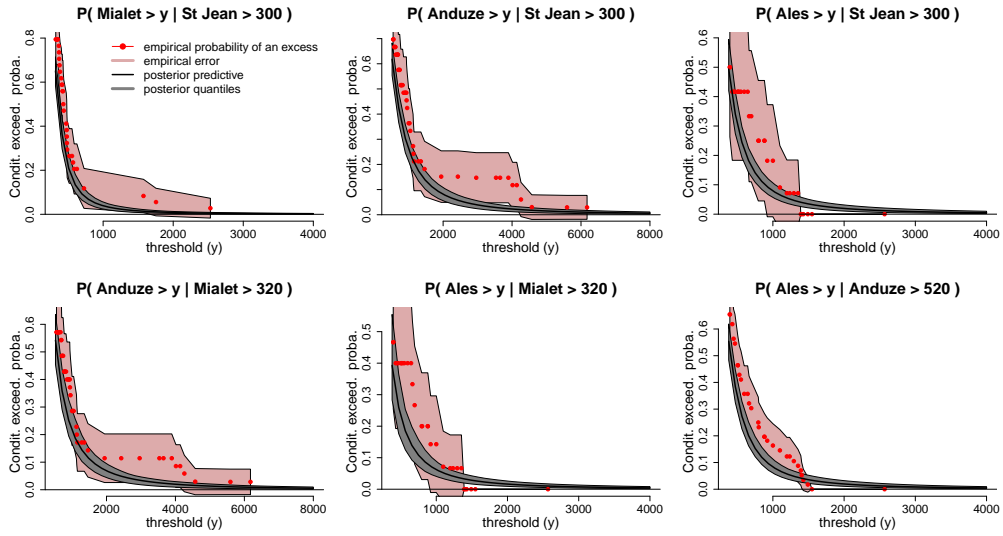


Figure 8: Conditional tail distributions. Black line and gray area: posterior mean estimate and posterior 90% credible intervals (posterior quantiles); red points: empirical tail function computed at the recorded points above threshold; pale red area: 90% Gaussian confidence intervals around the empirical estimates.

where X_i, X_j are the Fréchet-transformed variables at locations i and j . Since X_i and X_j are identically distributed, $\chi_{i,j} = \chi_{j,i}$. From its definition, $\chi_{i,j}$ is comprised between 0 and 1; small values indicate weak dependence at high levels whereas values close to 1 are characteristic of strong dependence. In the extreme case $\chi = 0$, the variables are asymptotically independent. In the case of Dirichlet mixtures, $\chi_{i,j}$ has an explicit expression (*Boldi and Davison, 2007*, eq. (9)). Figure 9 shows posterior box-plots of χ for the six pairs. The strength of the dependence and the amount of uncertainty varies from one pair to another, but mean estimates are overall large (greater than 0.4), indicating strong asymptotic dependence.

It is of interest to compare the pairwise dependence measures shown in Figure 7- Figure 9 with the properties of the catchments. The most dependent pair is Mialet - St Jean, which is not surprising considering that both catchments are relatively small, with a similar size, orientation and elevation range (Figure 1). Figure 7 also suggests peaky angular densities for the pairs St Jean - Anduze and Mialet - Anduze, which may be related to the fact that both St Jean and Mialet catchments are nested in Anduze catchment. Finally, the Ales catchment seems to stand apart, with much flatter angular densities. This may be due to the fact that its size is intermediate between St Jean / Mialet and Anduze, and that it is located on a distinct branch of the hydrologic network.

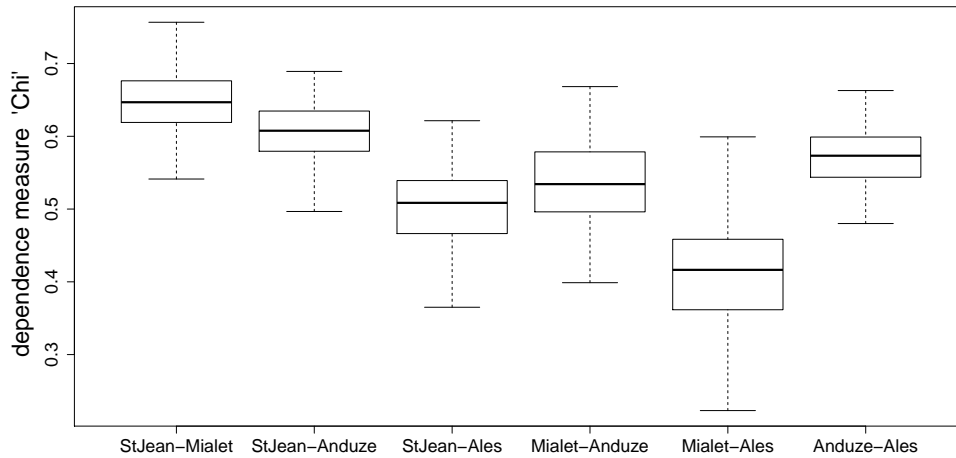


Figure 9: Dependence measure $\chi_{i,j}$ for the six pairs of locations: posterior box-plots.

In order to verify the consistency of those results with observed data, empirical quantities $P(X_i > x | X_j > x)$ have been computed and are displayed in Figure 10. More precisely, it is easy to see that

$$P(X_i > x | X_j > x) = P(Y_i^{\vee} > (F_i^X)^{-1} \circ F_j^X(y) | Y_j^{\vee} > y),$$

where F_i^X, F_j^X are the marginal *c.d.f.* for location i and j , and the Y_j^V, Y_i^V 's are the observed data (cluster maxima). In Figure 10, the conditioning thresholds y are the observed values of the conditioning variable Y_j^V above the initial threshold v_j , of which the estimated return period (abscissa of the red points) is taken as its mean estimate using the marginal parameter components of the posterior sample. For each such y , $(F_i^X)^{-1} \circ F_j^X(y)$ is estimated by its posterior mean value, again computed from the marginal posterior sample. Then, the conditional probability of an excess by Y_i^V (Y-axis value of the red points) is computed empirically. In theory, as the return period increases, the red points should come closer to the horizontal black line, which is the mean estimate of χ computed in the Dirichlet mixture dependence model, as in Figure 9. Note that in the Dirichlet model, the limiting value χ is already reached at finite levels because the conditional probability of an excess on the Fréchet scale, $P(X_i > x | X_j > x)$, is constant in x . On the contrary, in an asymptotically independent model, the conditional exceedance probability would be decreasing towards zero. Results in Figure 10 are comforting: the mean values of χ obtained from the Dirichlet model are within the error regions of the empirical estimates. The latter are very large, compared to the posterior quantiles from the Dirichlet mixture, which illustrates the usefulness of an extreme value model for computing conditional probabilities of an excess.

This result has implications for computing the return periods of joint excesses of high thresholds. Consider, for example, the 10 years marginal return levels at two stations, (q_1, q_2) . If the excesses above these thresholds were assumed to be independent, the probability of an excess above both levels within the same year would be approximately $(1/10)^2$, which yields a return period of 100 years. On the contrary, accounting for spatial dependence, for example between the two first stations (St Jean and Mialet), an estimate for the return period for a joint excess (within the same flood event) is : $10/\hat{\chi}_{1,2} = 10/0.645 = 15.5$ years.

5 Discussion

This section lists the limitations of the model used in this paper and discusses directions for improvement.

5.1 Other uncertainty sources: impact of systematic rating curve errors

The use of historical data allows extending the period of record and hence the availability of extreme flood events. However, historical data are also usually much more uncertain than recent systematic data, for two reasons: (i) the precision of historical water stages is limited; (ii) the transformation of these stage values into discharge values is generally based on a rating curve derived using a hydraulic model, which may induce large systematic errors.

The model used in the present paper ignores systematic errors (ii). This is because we focused on multivariate aspects through the use of the DM model to describe

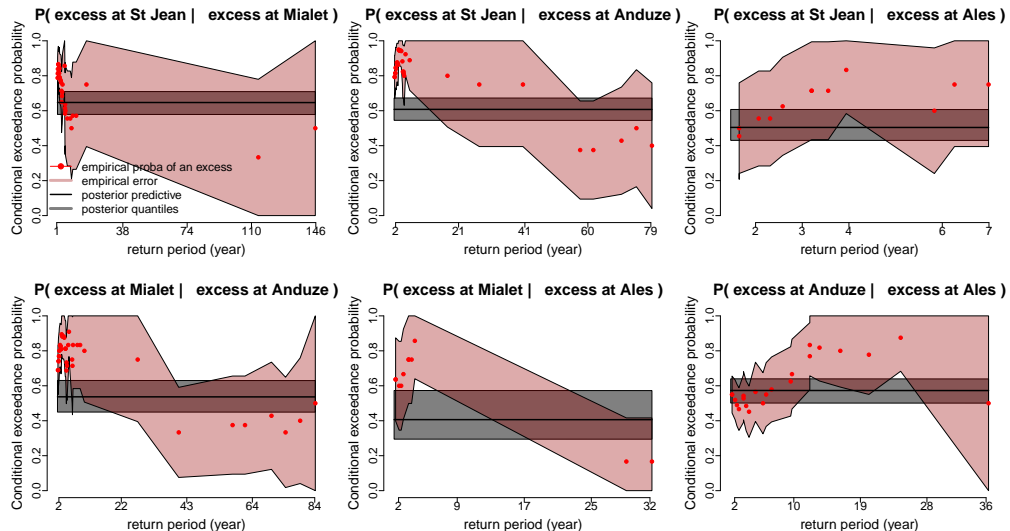


Figure 10: Observed conditional probability of exceedance of equally scaled thresholds. Red points: empirical estimates of conditional excesses; pale red regions, empirical standard error; horizontal black line and gray area, posterior mean and 0.05 – 0.95 quantiles of the theoretical value in the DM model.

intersite dependence. However, systematic errors may have a non-negligible impact on marginal quantile estimates, as discussed by *Neppel et al. (2010)*. Moreover, in a multivariate context, the impact of systematic errors on the estimation of the dependence structure is unclear at this stage and requires further evaluation. As an example, concerning the Anduze catchment, the empirical return level curve obtained with the historical dataset (black dots in Figure 6) has a non convex shape, which does not correspond to the expected behaviour of heavy tailed distributions. Also, again for the Anduze catchment, the empirical conditional exceedance probability curves (red dots in Figure 8, top-center and bottom-left panels) show a flat part, which is quite unrealistic. This may partly explain why the model fit in Anduze is poorer than for the other stations. Future work will therefore aim at incorporating an explicit treatment of systematic errors, using models such as those discussed by *Reis and Stedinger (2005)* or *Neppel et al. (2010)*.

Another potential source of uncertainty is the estimation of marginal threshold exceedance probabilities (parameter ζ , see section 3.1). In this work, it has been decided not to consider the impact of these errors, since their relative magnitude is moderate enough, which makes us believe that the main source of uncertainty concerns the rating curves. It would however certainly be feasible to account for those, *e.g.* by treating the exceedance probability as an additional parameter to be estimated in the MCMC scheme. This would bring d additional parameters in the procedure, which is not unreasonable compared to the large number of parameters for the dependence

structure.

5.2 Regional shape

As mentioned in Section 14, the variability across the different sites of the posterior distributions of marginal quantities suggest a more thorough investigation concerning the hypothesis of a common shape parameter. One possible improvement of the likelihood ratio test procedure adopted here would be to use a complexity penalty criterion such as the DIC (Deviance Information Criterion) or one of its variants, see *e.g.* Spiegelhalter *et al.* (2014) or Celeux *et al.* (2006) and the references therein. Indeed, the latter criterion does not require precise knowledge of the effective number of parameters, which is a valuable feature in our context, where the number of mixture components, thus the number of parameters is let free to vary.

5.3 Comparing several models for intersite dependence

The DM model used in this paper to describe intersite dependence is a valid dependence model according to multivariate extreme value theory (MEVT). Many alternative approaches, not necessarily MEVT-compatible, have been proposed in the hydrological literature on regional estimation methods. Such approaches include simply ignoring dependence (*e.g.* Dalrymple, 1960), the concept of 'equivalent number of sites' (Reed *et al.*, 1999) or the use of copulas (*e.g.* Renard, 2011). This raises the question of the influence of the approach used to describe dependence on the following estimates:

- Marginal estimates, typically quantile estimates at each site. While the impact of ignoring dependence altogether has been studied by several authors (Stedinger, 1983; Hosking and Wallis, 1988; Madsen and Rosbjerg, 1997; Renard and Lang, 2007), the impact of alternative dependence models is less clear. In particular, since marginal estimates do not directly use the dependence model, it remains to be established whether or not different dependence models (*e.g.* asymptotically dependent vs. asymptotically independent) yield significantly different results.
- Joint or conditional estimates, as illustrated in Figures 3, 8 and 10 for instance. The dependence model obviously plays a much more important role in this case.

Such comparison has not been attempted in this paper because the use of censored historical data makes the application of standard methods like copulas much more challenging.

5.4 The treatment of dependence in a highly dimensional context

As illustrated in the case study, the DM model is applicable in moderate dimension ($d = 4$ in this particular case study, dimensions up to $d \simeq 10$ remain realistic). This

already covers a range of interesting potential applications beyond the multisite context presented here. In particular, the DM model could be applied in the context of characterizing flood or drought events using several variables (typically, peak-volume-duration variables, as described by e.g. *Favre et al.* (2004) and *Genest and Favre* (2007) for floods and as reviewed by *Mishra and Singh* (2011) for droughts).

However, such semi-parametric approach is admittedly not geared toward highly-dimensional contexts (e.g. spatial rainfall using dozens or hundreds of rain gauges, or gridded data sets). Practical approaches for highly-dimensional multivariate extremes have been mostly proposed in the context of block maxima, using the theory of max-stable processes (*De Haan*, 1984; *Smith*, 1990; *Schlather*, 2002; *Westra and Sisson*, 2011). Estimation procedures e.g. using composite likelihood methods exist for such processes (*Padoan et al.*, 2010), along with descriptive tools e.g. to define and estimate extremal dependence coefficients such as the madogram (*Cooley et al.*, 2006). However, the development of models adapted to peaks-over-threshold is still an area of active research in a highly-dimensional spatial context and full modeling (which would e.g. allow simulation of joint excesses) remain elusive. Recent theoretical advances (*Ferreira and de Haan*, 2012; *Dombry and Ribatet*, 2013) give cause to hope for, and expect, future development of spatial peaks-over-threshold models.

6 Conclusion

This paper illustrates the use of a multivariate peaks-over-threshold model to combine regional estimation and historical floods. This model is based on a semi-parametric Dirichlet Mixture to describe intersite dependence, while Generalized Pareto distributions are used for margins. A data augmentation scheme is used to enable the inclusion of censored historical flood data. The model is applied to four catchments in Southern France where historical flood data are available.

The first objective of this case study was to assess the relative impact of regional and historical information on marginal quantile estimates at each site. The main results can be summarized as follows:

- Over the four considered versions of the model, the version ignoring historical floods and performing local estimation yields estimates that may strongly differ from the other versions. The three other versions (which either use historical floods or perform regional estimation or both) yield more consistent estimates. This illustrates the benefit of extending the at-site sample using either historical or regional information, or both.
- Compared with the most complete version of the model (which enables both historical floods and regional estimation), the version only implementing regional estimation (but ignoring historical floods) yields smaller estimates of the shape parameter, and hence smaller quantiles. This result is likely specific to this particular data set, for which many large floods have been recorded during the historical period.

- Compared with the most complete version of the model, the version using historical floods but implementing local estimation yields higher quantiles for three catchments but lower quantiles on the fourth.
- The uncertainty in parameter estimates generally decreases when more information (regional, historical or both) is included in the inference. However, this does not necessarily result in smaller uncertainty in quantile estimates. This is because this uncertainty does not only depends on the uncertainty in parameter estimates, but also on the value taken by the parameters. In particular, a precise but large shape parameter may result in more uncertain quantiles than a more imprecise but smaller shape parameter.

The second objective was to investigate the nature of asymptotic dependence in this flood data set, by taking advantage of the existence of extremely high joint exceedances in the historical data. Results in terms of predictive angular density suggest the existence of such dependence between every pairs of catchments of asymmetrical nature: some pairs are more dependent than others at asymptotic levels. In addition, the Dirichlet Mixture model allows to compute bi-variate conditional probabilities of large threshold exceedances, which are poorly estimated with empirical methods. The limiting values of the conditional probabilities, theoretically obtained with increasing thresholds, are substantially non zero (they range between 0.4 and 0.65), which confirms the strength and the asymmetry of pairwise asymptotic dependence for this data set and induces multivariate return periods much shorter than they would be in the asymptotically independent case.

Acknowledgments

The data and the code involved in this work are available from the authors upon request. The first author would like to thank Anne-Laure Fougères and Philippe Naveau for their useful advice. Part of this work has been supported by the EU-FP7 ACQWA Project (www.acqwa.ch), by the PEPER-GIS project, by the ANR (MOPERA, McSim, StaRMIP) and by the MIRACCLE-GICC project.

References

- Beirlant, J., Y. Goegebeur, J. Segers, and J. Teugels (2004), *Statistics of extremes: Theory and applications*, John Wiley & Sons: New York.
- Boldi, M.-O., and A. C. Davison (2007), A mixture model for multivariate extremes, *Journal of the Royal Statistical Society: Series B (Statistical Methodology)*, 69(2), 217–229, doi:10.1111/j.1467-9868.2007.00585.x.
- Celeux, G., F. Forbes, C. P. Robert, D. M. Titterton, et al. (2006), Deviance information criteria for missing data models, *Bayesian analysis*, 1(4), 651–673.

- Chi Cong, N., O. Payraastre, and E. Gaume (2015), Reducing uncertainties on low-probability flood peak discharge quantile estimates: comparison of historical and/or regional approaches, *Houille Blanche-Revue Internationale De L Eau*, (3), 64–71, times Cited: 0.
- Coles, S. (2001), *An introduction to statistical modeling of extreme values*, Springer Verlag.
- Coles, S., and J. Tawn (1991), Modeling extreme multivariate events, *JR Statist. Soc. B*, 53, 377–392.
- Coles, S., J. Heffernan, and J. A. Tawn (1999), Dependence measures for extreme value analyses, *Extremes*, 2, 339–365.
- Cooley, D., P. Naveau, and P. Poncet (2006), Variograms for spatial max-stable random fields, in *Dependence in probability and statistics*, pp. 373–390, Springer.
- Cooley, D., R. Davis, and P. Naveau (2010), The pairwise beta distribution: A flexible parametric multivariate model for extremes, *Journal of Multivariate Analysis*, 101(9), 2103–2117.
- Dalrymple, T. (1960), Flood frequency analyses, *Water-supply paper 1543-A*.
- Davison, A., and R. Smith (1990), Models for exceedances over high thresholds, *Journal of the Royal Statistical Society. Series B (Methodological)*, pp. 393–442.
- Davison, A. C., R. Huser, and E. Thibaud (2013), Geostatistics of dependent and asymptotically independent extremes, *Mathematical Geosciences*, 45(5), 511–529.
- De Haan, L. (1984), A spectral representation for max-stable processes, *The annals of probability*, pp. 1194–1204.
- De Haan, L., and J. De Ronde (1998), Sea and wind: Multivariate extremes at work, *Extremes*, 1, 7–45.
- Dombry, C., and M. Ribatet (2013), Functional regular variations, pareto processes and peaks over threshold.
- Favre, A. C., S. El Adlouni, L. Perreault, N. Thiémonge, and B. Bobee (2004), Multivariate hydrological frequency analysis using copulas, *Water Resources Research*, 40(1).
- Fawcett, L., and D. Walshaw (2007), Improved estimation for temporally clustered extremes, *Environmetrics*, 18(2), 173–188.
- Ferreira, A., and L. de Haan (2012), The generalized pareto process; with a view towards application and simulation, *arXiv preprint arXiv:1203.2551v2*.
- Ferro, C., and J. Segers (2003), Inference for clusters of extreme values, *Journal of the Royal Statistical Society: Series B (Statistical Methodology)*, 65(2), 545–556.

- Fougères, A.-L., C. Mercadier, and P. Nolan, John (2013), Dense classes of multivariate extreme value distributions, *Journal of Multivariate Analysis*, *116*, 109–129, doi: 10.1016/j.jmva.2012.11.015.
- Gaume, E., L. Gaal, A. Viglione, J. Szolgay, S. Kohnova, and G. Bloschl (2010), Bayesian mcmc approach to regional flood frequency analyses involving extraordinary flood events at ungauged sites, *Journal of Hydrology*, *394*, 101–117.
- Gelman, A., and D. Rubin (1992), Inference from iterative simulation using multiple sequences, *Statistical science*, pp. 457–472.
- Genest, C., and A. C. Favre (2007), Metaelliptical copulas and their use in frequency analysis of multivariate hydrological data, *Water Resources Research*, *43*.
- Ghizzoni, T., G. Roth, and R. Rudari (2012), Multisite flooding hazard assessment in the upper mississippi river, *Journal of Hydrology*, *412*, 101–113.
- Gumbel, E. (1960), Distributions des valeurs extrêmes en plusieurs dimensions, *Publ. Inst. Statist. Univ. Paris*, *9*, 171–173.
- Heffernan, J., and J. Tawn (2004), A conditional approach for multivariate extreme values (with discussion), *Journal of the Royal Statistical Society: Series B (Statistical Methodology)*, *66*(3), 497–546.
- Heffernan, J. E., and S. I. Resnick (2007), Limit laws for random vectors with an extreme component, *The Annals of Applied Probability*, pp. 537–571.
- Heidelberger, P., and P. Welch (1983), Simulation run length control in the presence of an initial transient, *Operations Research*, pp. 1109–1144.
- Hosking, J. (1985), Maximum-likelihood estimation of the parameters of the generalized extreme-value distribution, *Applied Statistics*, *34*, 301–310.
- Hosking, J., and J. R. Wallis (1987), Parameter and quantile estimation for the generalized pareto distribution, *Technometrics*, *29*(3), 339–349.
- Hosking, J., and J. R. Wallis (1988), The effect of intersite dependence on regional flood frequency analysis, *Water Resources Research*, *24*, 588–600.
- Hosking, J., and J. R. Wallis (1997), *Regional Frequency Analysis: an approach based on L-Moments*, Cambridge University Press, Cambridge, UK.
- Huser, R., and A. C. Davison (2014), Space–time modelling of extreme events, *Journal of the Royal Statistical Society: Series B (Statistical Methodology)*, *76*(2), 439–461, doi:10.1111/rssb.12035.
- Jin, M., and J. R. Stedinger (1989), Flood frequency analysis with regional and historical information, *Water Resources Research*, *25*(5), 925–936.

- Joe, H., R. L. Smith, and I. Weissman (1992), Bivariate threshold methods for extremes, *Journal of the Royal Statistical Society. Series B (Methodological)*, pp. 171–183.
- Katz, R. W., M. B. Parlange, and P. Naveau (2002), Statistics of extremes in hydrology, *Advances in water resources*, *25*(8), 1287–1304.
- Keef, C., C. Svensson, and J. A. Tawn (2009), Spatial dependence in extreme river flows and precipitation for great britain, *Journal of Hydrology*, *378*(3–4), 240 – 252, doi:http://dx.doi.org/10.1016/j.jhydrol.2009.09.026.
- Kochanek, K., B. Renard, P. Arnaud, Y. Aubert, M. Lang, T. Cipriani, and E. Sauquet (2014), A data-based comparison of flood frequency analysis methods used in france, *Nat. Hazards Earth Syst. Sci.*, *14*(2), 295–308, nHESS.
- Lang, M., T. Ouarda, and B. Bobee (1999), Towards operational guidelines for over-threshold modeling, *Journal of Hydrology*, *225*, 103–117.
- Leadbetter, M. (1983), Extremes and local dependence in stationary sequences, *Probability Theory and Related Fields*, *65*(2), 291–306.
- Ledford, A., and J. Tawn (1996), Statistics for near independence in multivariate extreme values, *Biometrika*, *83*(1), 169–187.
- Machado, M., B. Botero, J. López, F. Francés, A. Díez-Herrero, and G. Benito (2015), Flood frequency analysis of historical flood data under stationary and non-stationary modelling, *Hydrology and Earth System Sciences Discussions*, *12*(1), 525–568.
- Madsen, H., and D. Rosbjerg (1997), The partial duration series method in regional index-flood modeling, *Water Resources Research*, *33*(4), 737–746.
- Madsen, H., P. F. Rasmussen, and D. Rosbjerg (1997a), Comparison of annual maximum series and partial duration series methods for modeling extreme hydrologic events .1. at-site modeling, *Water Resources Research*, *33*(4), 747–757.
- Madsen, H., C. P. Pearson, and D. Rosbjerg (1997b), Comparison of annual maximum series and partial duration series methods for modeling extreme hydrologic events .2. regional modeling, *Water Resources Research*, *33*(4), 759–769.
- Mishra, A. K., and V. P. Singh (2011), Drought modeling – a review, *Journal of Hydrology*, *403*(1–2), 157–175.
- Nadarajah, S. (2001), Multivariate declustering techniques, *Environmetrics*, *12*(4), 357–365.
- Naulet, R., M. Lang, T. B. Ouarda, D. Coeur, B. Bobée, A. Recking, and D. Moussay (2005), Flood frequency analysis on the ardèche river using french documentary sources from the last two centuries, *Journal of Hydrology*, *313*(1), 58–78.

- Neppel, L., P. Arnaud, and J. Lavabre (2007), Extreme rainfall mapping: Comparison between two approaches in the mediterranean area, *Comptes Rendus Geoscience*, 339(13), 820–830.
- Neppel, L., B. Renard, M. Lang, P. Ayrat, D. Coeur, E. Gaume, N. Jacob, O. Payrastre, K. Pobanz, and F. Vinet (2010), Flood frequency analysis using historical data: accounting for random and systematic errors, *Hydrological Sciences Journal—Journal des Sciences Hydrologiques*, 55(2), 192–208.
- Neppel, L., P. Arnaud, F. Borchi, J. Carreau, F. Garavaglia, M. Lang, E. Paquet, B. Renard, J.-M. Soubeyroux, and J.-M. Veysseire (2014), Résultats du projet extraflo sur la comparaison des méthodes d’estimation des pluies extrêmes en france, *La houille blanche*, (2), 14–19.
- O’Connel, D., D. Ostenaar, D. Levisch, and R. Klinger (2002), Bayesian flood frequency analysis with paleohydrologic bound data, *Water Resources Research*, 38(5).
- Padoan, S. A., M. Ribatet, and S. A. Sisson (2010), Likelihood-based inference for max-stable processes, *Journal of the American Statistical Association*, 105(489).
- Parent, E., and J. Bernier (2003), Bayesian pot modeling for historical data, *Journal of hydrology*, 274, 95–108.
- Payrastre, O., E. Gaume, and H. Andrieu (2011), Usefulness of historical information for flood frequency analyses: Developments based on a case study, *Water Resources Research*, 47.
- Reed, D. W., D. S. Faulkner, and E. J. Stewart (1999), The forgen method of rainfall growth estimation - ii: Description, *Hydrology and Earth System Sciences*, 3(2), 197–203.
- Reich, B. J., and B. A. Shaby (2012), A hierarchical max-stable spatial model for extreme precipitation, *The annals of applied statistics*, 6(4), 1430.
- Reis, D., and J. R. Stedinger (2005), Bayesian mcmc flood frequency analysis with historical information, *Journal of Hydrology*, 313(1-2), 97–116.
- Renard, B. (2011), A bayesian hierarchical approach to regional frequency analysis, *Water Resources Research*, 47.
- Renard, B., and M. Lang (2007), Use of a gaussian copula for multivariate extreme value analysis: some case studies in hydrology, *Advances in Water Resources*, 30(4), 897–912.
- Resnick, S. (1987), *Extreme values, regular variation, and point processes, volume 4 of Applied Probability. A Series of the Applied Probability Trust*, Springer-Verlag, New York.
- Resnick, S. (2007), *Heavy-Tail Phenomena: Probabilistic and Statistical Modeling*, Springer Series in Operations Research and Financial Engineering.

- Ribatet, M., T. B. Ouarda, E. Sauquet, and J.-M. Gresillon (2009), Modeling all exceedances above a threshold using an extremal dependence structure: Inferences on several flood characteristics, *Water Resources Research*, *45*(3).
- Ribereau, P., P. Naveau, and A. Guillou (2011), A note of caution when interpreting parameters of the distribution of excesses, *Advances in Water Resources*, *34*(10), 1215–1221.
- Sabourin, A. (2015), Semi-parametric modeling of excesses above high multivariate thresholds with censored data, *Journal of Multivariate Analysis*, *136*, 126–146.
- Sabourin, A., and P. Naveau (2014), Bayesian dirichlet mixture model for multivariate extremes: A re-parametrization, *Computational Statistics & Data Analysis*, *71*, 542–567.
- Sabourin, A., P. Naveau, and A.-L. Fougères (2013), Bayesian model averaging for multivariate extremes, *Extremes*, *16*(3), 325–350.
- Salvadori, G., and C. De Michele (2010), Multivariate multiparameter extreme value models and return periods: A copula approach, *Water Resources Research*, *46*(10), n/a–n/a, doi:10.1029/2009WR009040.
- Schlather, M. (2002), Models for stationary max-stable random fields, *Extremes*, *5*(1), 33–44.
- Serinaldi, F., A. Bárdossy, and C. G. Kilsby (2014), Upper tail dependence in rainfall extremes: would we know it if we saw it?, *Stochastic Environmental Research and Risk Assessment*, pp. 1–23.
- Smith, R. (1994), Multivariate threshold methods, *Extreme Value Theory and Applications*, *1*, 225–248.
- Smith, R., J. Tawn, and S. Coles (1997), Markov chain models for threshold exceedances, *Biometrika*, *84*(2), 249–268.
- Smith, R. L. (1990), Max-stable processes and spatial extremes, *Unpublished manuscript, Univer.*
- Spiegelhalter, D. J., N. G. Best, B. P. Carlin, and A. Linde (2014), The deviance information criterion: 12 years on, *Journal of the Royal Statistical Society: Series B (Statistical Methodology)*, *76*(3), 485–493.
- Stedinger, J. R. (1983), Estimating a regional flood frequency distribution, *Water Resources Research*, *19*, 503–510.
- Stedinger, J. R., and T. A. Cohn (1986), Flood frequency-analysis with historical and paleoflood information, *Water Resources Research*, *22*(5), 785–793.
- Stephenson, A. (2003), Simulating multivariate extreme value distributions of logistic type, *Extremes*, *6*(1), 49–59.

- Stephenson, A. (2009), High-dimensional parametric modelling of multivariate extreme events, *Australian & New Zealand Journal of Statistics*, 51(1), 77–88.
- Sun, X., M. Thyer, B. Renard, and M. Lang (2014), A general regional frequency analysis framework for quantifying local-scale climate effects: A case study of enso effects on southeast queensland rainfall, *Journal of Hydrology*, 512, 53–68.
- Tanner, M., and W. Wong (1987), The calculation of posterior distributions by data augmentation, *Journal of the American Statistical Association*, 82(398), 528–540.
- Tasker, G. D., and J. R. Stedinger (1987), Regional regression of flood characteristics employing historical information, *Journal of Hydrology*, 96, 255–264.
- Tasker, G. D., and J. R. Stedinger (1989), An operational gls model for hydrologic regression, *Journal of Hydrology*, 111, 361:375.
- Van Dyk, D., and X. Meng (2001), The art of data augmentation, *Journal of Computational and Graphical Statistics*, 10(1), 1–50.
- Viglione, A., R. Merz, J. L. Salinas, and G. Blöschl (2013), Flood frequency hydrology: 3. a bayesian analysis, *Water Resources Research*, 49(2), 675–692.
- Wadsworth, J. L., and J. A. Tawn (2012), Dependence modelling for spatial extremes, *Biometrika*, p. asr080.
- Weiss, J., P. Bernardara, and M. Benoit (2014), Modeling intersite dependence for regional frequency analysis of extreme marine events, *Water Resources Research*, 50(7), 5926–5940.
- Westra, S., and S. A. Sisson (2011), Detection of non-stationarity in precipitation extremes using a max-stable process model, *Journal of Hydrology*, 406(1), 119–128.